Environmental Earth Sciences (2021) 80:309
https://doi.org/10.1007/s12665-021-09453-5

ORIGINAL ARTICLE

Mechanical and energy characteristics of coal–rock composite sample with different height ratios: a numerical study based on particle flow code

Qing Ma[1,2,3] · Yun-liang Tan[1,2] · Xue-sheng Liu[1,2] · Zeng-hui Zhao[1,2] · De-yuan Fan[1,2]

Received: 21 June 2020 / Accepted: 22 January 2021 / Published online: 7 April 2021

Abstract

To explore the differences in mechanical and energy evolution characteristics of coal–rock composite samples with different coal–rock height ratios, uniaxial compression tests of coal–rock composite samples with height ratios ranging from 4:1 to 1:4 were conducted by PFC software. A total of 7 PFC models were built and calculated. Results show that the smaller coal–rock height ratios lead to the higher elastic modulus and higher peak strength, both following exponential relationships with coal–rock height ratios, while the peak strain decreases linearly with the decrease of coal–rock height ratios. When the coal–rock height ratios decrease from 4:1 to 1:3, the fragmentation degree of coal body decreases gradually, and the failure modes are mainly of "V" type. And when the ratio is reduced to 1:4, failure mode is no longer of "V" type, the degree of coal body breaking becomes larger, and the part of rock body in the composites is also damaged. With the decrease of coal–rock height ratios, number of acoustic emission events of the composites increase first and then decrease. And U, U_e and U_d at different coal–rock height ratios exhibited similar trends, all of which increase slowly first, fast afterwards and very sharply at the peak stress points. At the peak stress point, the values of total input energy (U_A) and dissipative energy ($U_A d$) decrease firstly then increase as the coal-rock height ratios decreases and the value of elastic strain energy ($U_A e$) decrease as coal-rock height ratios decreases. While the decrease of both U_A and $U_A d$ are larger than $U_A e$. These results can provide a useful reference for safe and efficient exploitation of coal resources.

Keywords Coal–rock composite sample · Acoustic emission · Deformation and failure · Height ratios · Energy evolution

✉ Yun-liang Tan
yunliangtan@163.com

✉ Xue-sheng Liu
xuesheng1134@163.com

Qing Ma
Qingma@mines.edu

Zeng-hui Zhao
tgzyzzh@163.com

De-yuan Fan
2460791279@qq.com

1 State Key Laboratory of Mining Disaster Prevention and Control Co-Founded by Shandong Province and the Ministry of Science and Technology, Shandong University of Science and Technology, Qingdao 266590, China

2 College of Energy and Mining Engineering, Shandong University of Science and Technology, Qingdao 266590, China

3 Department of Mining Engineering, Colorado School of Mines, 1500 Illinois Str., Golden, CO 80401, USA

Introduction

Coal is still the main energy source in China (As shown in Fig. 1) (CESA 2019; Cheng et al. 2019; Tan et al. 2019a, b). As coal mining practice is speeding up from shallow to deep, different disasters are also increasing (Zhang et al. 2014; Xie 2017; Tan et al. 2019a, b). It is found that the occurrence of roof fall, coal explosion and rock burst is not only related to coal and rock itself, but also closely related to the geological structure, occurrence characteristics, and combination of coal seam and rock stratum (Ward 1984; Kenetia and Sainsbury, 2018; Sun et al. 2018; Thomas 2002; Tan et al. 2018; Ning et al. 2020; Wang et al. 2020; Zhang et al. 2020a, b; Wang and Tian 2018). So the mechanical and deformation characteristics of the composite structure formed by coal and rock are very important for the safe production of coal mines. Many studies also found that height ratios, interface, strength of coal or rock, strain rate of loading, loading path and confining pressure, etc. have an important influence on

Fig. 1 Proportion of coal production of major coal producing countries in the world in 2016 and China's energy structure and world's energy structure (CESA 2019; Cheng et al. 2019)

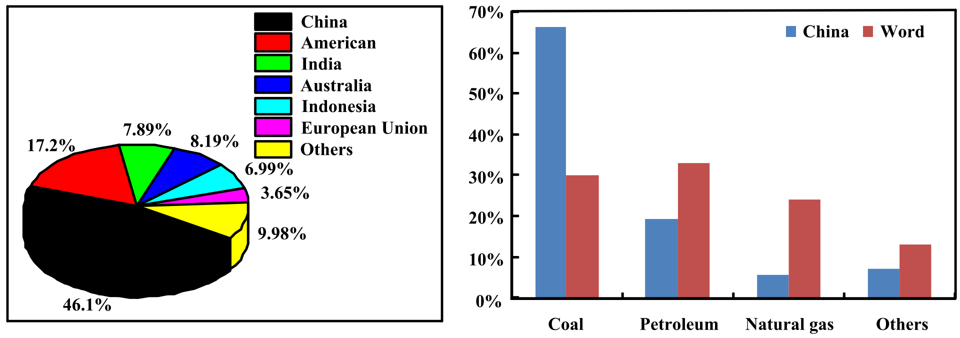

stability of composite coal–rock mass (Zhang et al. 2016; Liu et al. 2018; Tan et al. 2018; Zhao et al. 2015; Chen et al. 2019). Therefore, a comprehensive understanding of mechanical characteristics of coal–rock composites is very essential to safe exploitation of coal resources.

In recent years, many researches focus on coal–rock composite structures, and some achievements have been obtained. For instance, the influence of interface (Zhao et al. 2015, 2016; Hu et al. 2019; Mishra and Verma 2015), strength of coal or rock (Zhao et al. 2020), strain rate of loading (Chen et al. 2019), loading path (Zhao et al. 2021; Liu et al. 2016; Chen et al. 2019) and confining pressure (Zuo et al. 2011) on the mechanical characteristics of coal–rock composites have been carried out through a large number of numerical simulations and indoor rock mechanical tests. And during the mining practice, thickness of coal or rock mass can vary greatly during different segments of the same mining area (Álvarez-Fernández et al. 2009; Zhang and Dou 2006; Chen et al. 2016). Experiments have been carried out on coal–rock height ratios and other factors on the mechanical behavior of coal–rock composites, such as uniaxial compression tests (Ma et al. 2020; Chen et al. 2018; Poulsen et al. 2014), triaxial compression tests (Wang et al. 2017) and Split-Hopkinson pressure bar apparatus dynamic tests (Gong et al. 2018; Liu et al. 2014). In addition, Yin et al. (2019) made a preliminary study on mechanical properties of coal–rock composites with different ratios through laboratory rock mechanics test. Tan et al. (2016) studied acoustic emission (AE) characteristics and rock burst tendency of coal–rock combination bodies through numerical simulation test. Zhao et al. (2008) studied precursory information of coal rock combination by infrared thermal image and acoustic emission. And some researchers have also studied the influence of water and temperature on mechanical characteristics of coal–rock composites with different height ratios (Huang et al. 2018; Yang et al. 2016). All of these studies have achieved a lot of beneficial results on the influence of different heights on the mechanical properties of coal–rock composites from different aspects.

However, in comparison, these studies fail to consider the influence of different coal–rock height ratios on energy evolution behavior of coal–rock composites. Given this, this paper presents some results of uniaxial compression tests on coal–rock composites at different coal-rock height ratios with numerical simulation software PFC2D, aiming to study the effect of coal–rock height ratios on mechanical properties, AE and energy evolution characteristics.

Coal–rock composites in engineering and mechanical model

The rock layer histogram and the mining schematic diagram of the working face are shown in Fig. 2. The occurrence of such disasters as rock burst and roof caving in mining engineering is not only related to the impact tendency of coal and rock mass itself, but also closely related to the mineral composition, geological structure, occurrence characteristics and composite form of coal and rock mass (Ward 1984; Kenetia and Sainsbury 2018; Thomas 2002; Tan et al. 2018; Wang et al. 2020; Wang and Tian 2018). The failure of coal and rock is a nonlinear instability phenomenon driven by energy (Xie et al. 2005). So if the energy evolution characteristics during the deformation and failure of coal–rock composites can be analyzed in detail, it is possible to get a closer understanding of the causes of failure of coal–rock composites. And as can be seen from Fig. 2b, during mining process, thickness of coal or rock mass can vary during different segments of the same mining area (Álvarez-Fernández et al. 2009; Zhang and Dou 2006; Chen et al. 2016). Therefore, it is necessary to study the mechanical and energy evolution characteristics of coal–rock composites under different coal–rock height ratios.

Numerical simulation

Linear parallel bond model and AE Simulation by PFC

Since principle of the parallel bonding model (BPM) has been introduced a lot in other papers (Cundall and Strack 1980; Cho et al. 2007), this article only briefly introduces

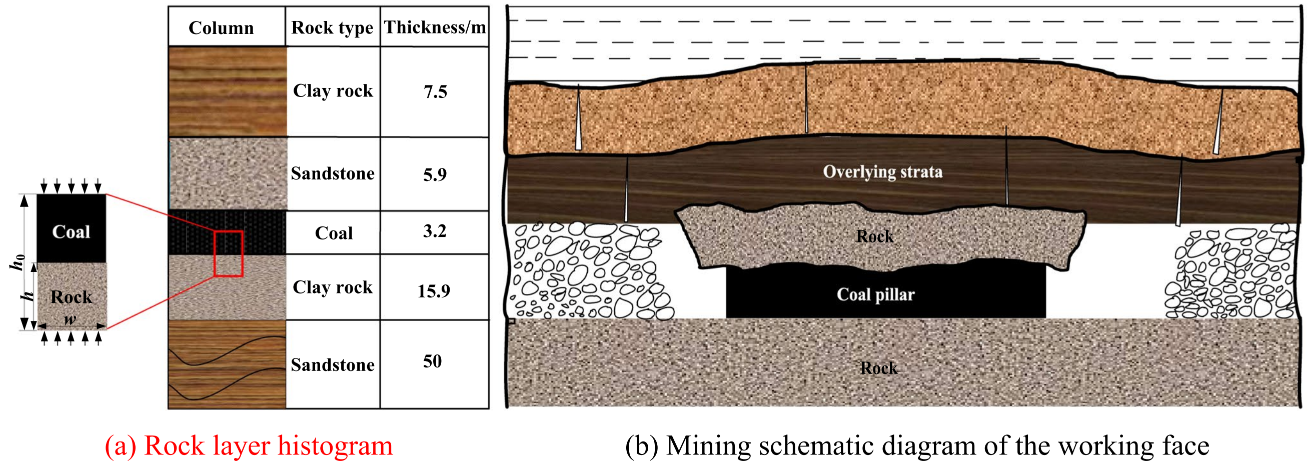

Fig. 2 Rock layer histogram and the mining schematic diagram of the working face (Chen et al. 2018; Ma et al. 2020)

main characteristics of the BPM used in this paper. In PFC program, interaction between particles is expressed by built-in multiple contact constitutive models. Among them, linear contact bond model (Linearcbond) and linear parallel bond model (Linearpbond) are most widely used (Cundall and Strack 1980; Cho et al. 2007). Linearcbond cannot resist bending moments. But Linearpbond can transfer forces and moments between different entities and can also resist shear and stretching caused by external forces (Fig. 3). As remarked by Cho et al. (2007), the parallel bond model is a more realistic bond model for rock-like materials whereby the bonds may break in either tension or shearing with an associated reduction in stiffness. Therefore, this article uses Linearpbond model to conduct theoretical research. The main micro parameters of simulated materials in the Linearpbond are shown in Table 1 (Cundall and Strack 1980; Cho et al. 2007).

AE refers to the phenomenon of elastic cracks and internal strain energy release during internal crack formation and expansion during material's deformation and failure. AE detection technology is a dynamic detection technology. It can reflect formation and expansion of internal cracks in the process of material deformation and failure in real time (Zhang and Wong 2012; Lockner 1993; Mansurov 1994). The following are the main characteristic parameters of AE signals: ring count, event count, amplitude, energy, rise time, duration and effective value voltage. The AE event count can reflect crack formation and propagation of material. In

Fig. 3 Micro-parameters yielding process for micro-bonding (Cundall and Strack 1980; Zhang et al. 2020a, b)

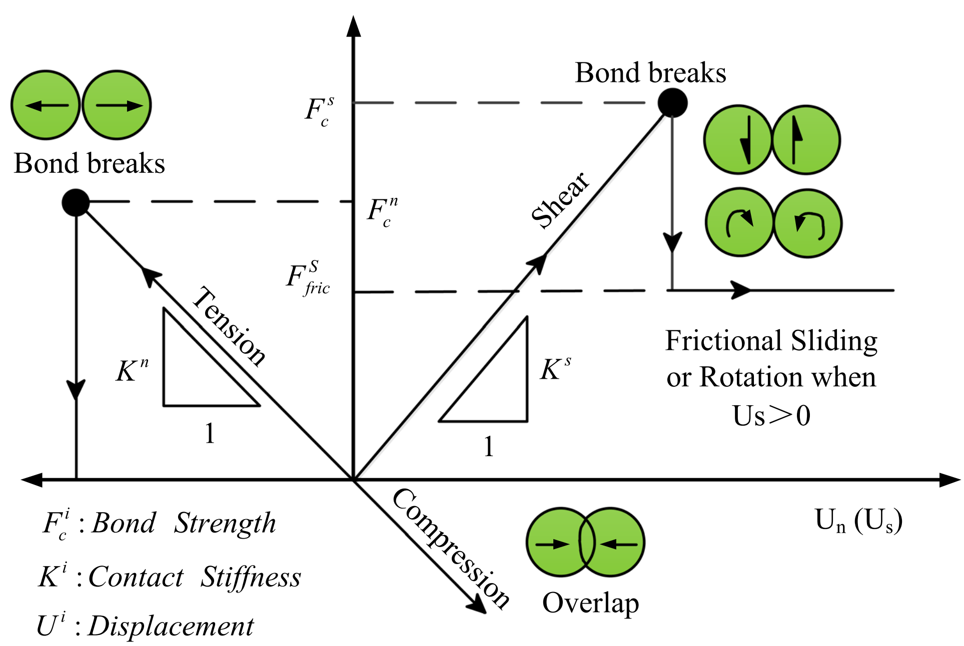

Table 1 The main micro parameters of simulated materials in Linearpbond model (Cundall and Strack 1980; Cho et al. 2007)

Particle parameters	Description	Parallel bond parameters	Description
R_{min}	Minimum particle size	$\bar{E}$	Parallel bonding elastic modulus
R_{max}/R_{min}	Particle size ratios	$\bar{K}_n / \bar{K}_s$	Parallel bond stiffness ratios
ρ	Particle density	$\bar{\sigma}_c$	Normal bond strength
E_c	Contact elastic modulus	$\bar{\tau}_c$	Tangential bond strength
Kn/Ks	Contact stiffness ratios		
μ	Particle friction coefficient		

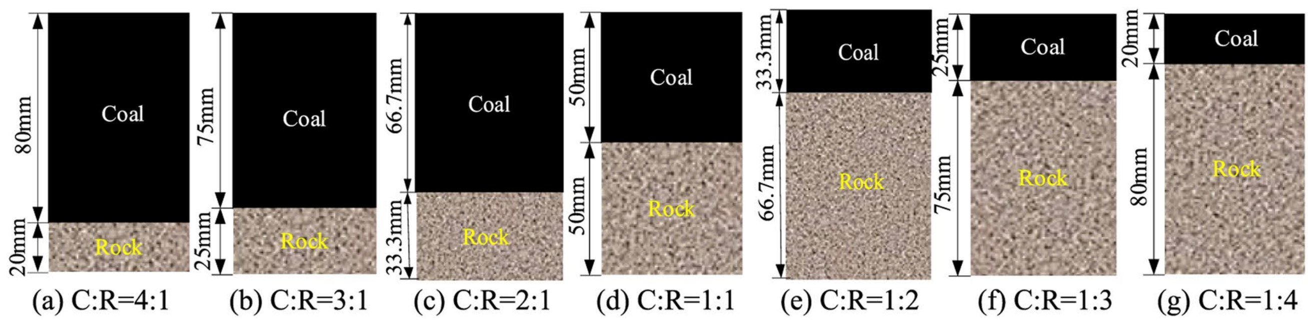

Fig. 4 Coal–rock composite samples in the physical experiments (C:R is coal and rock height ratio)

the BPM of PFC2D, each crack formation will form an AE pulse (Tan et al. 2016; Chen et al. 2019; Zhang et al. 2017). By recording number of cracks and post-processing of data during uniaxial compression of coal–rock composite samples with different coal–rock height ratios, it is possible to simulate calculation of AE events for coal–rock composite samples.

Model description

In the experiments conducted by Yin et al. (2019), standard cylinder coal–rock composite samples (50 mm × 100 mm) were tested under uniaxial compression (Fig. 4). In this study, the above physical experiments only change coal–rock height ratios and are repeated by numerical simulation.

This article uses particle flow software PFC2D to build a coal–rock composite sample model. First, a 50 × 100 mm standard rock sample model numerical test container is generated. The model is divided into two parts by adding a joint surface with the JSET command in the middle of the model. The upper and lower parts are used to simulate coal and rock, respectively. Then, micro parameters of the model are determined. For this simulation, meso-parameters of coal and rock in references (Guo et al. 2018; Zhao et al. 2016; Chen et al. 2019) are selected, as listed in Table 2. The numerical models of coal–rock composite samples are shown in Fig. 5. A total of 21,390 circular particles of different sizes were generated. The minimum particle radius is 0.2 mm and the maximum particle radius is 0.3 mm.

Table 2 Meso-mechanical parameters of coal and rock (Guo et al. 2018; Zhao et al. 2016; Chen et al. 2019)

Mechanical microparameters	Rock	Coal
ρ/kg·m^{-3}	2600	1800
R_{min}/mm	0.2	0.2
R_{max}/R_{min}	1.5	1.5
E_c/GPa	12	4
K_n/K_s	2.5	2.5
$\bar{E}$/GPa	12	4
$\bar{K}_n / \bar{K}_s$	2.5	2.5
$\bar{\sigma}_c$/MPa	45	15
$\bar{\tau}_c$/MPa	45	15
μ	0.5	0.5

Numerical test scheme

The current simulation work is aimed to study the coal–rock height ratios on mechanical behavior of coal–rock composite samples under uniaxial compression. A total of seven simulations of uniaxial compression tests on coal–rock composite

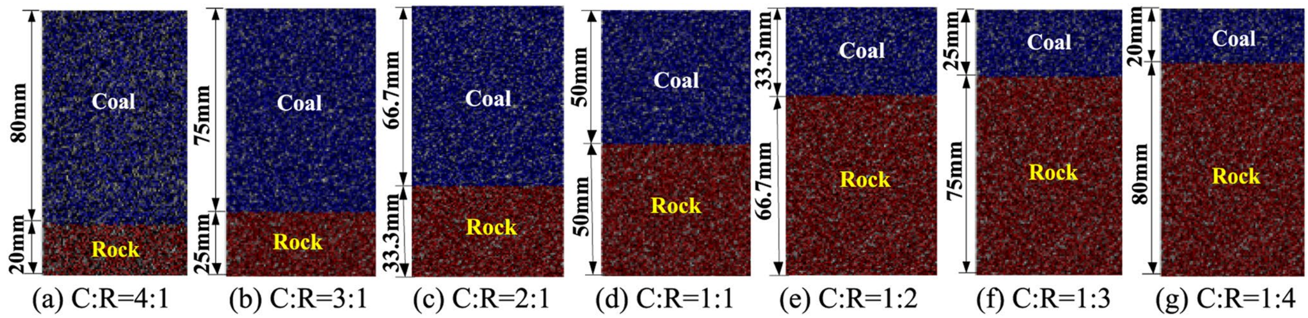

Fig. 5 The numerical models of coal–rock composite samples with different coal–rock height ratios

samples were performed over a range of coal–rock height ratios of 4:1, 3:1, 2:1, 1:1, 1:2, 1:3, 1:4. Loading is performed by moving upper and lower walls. And loading rate is 0.05 m/s. The simulation process of coal–rock composite samples with different coal–rock height ratios is divided into following four steps:

Firstly, the coal-rock height ratio of 4:1 is tested. The upper wall remains stationary, and the lower wall rises at a upward speed of 0.05m/s until the sample is broken;

second, record the stress–strain correspondence during sample loading process, as well as crack development and failure characteristics of the sample;

then, change the coal–rock height ratios, take 3:1, 2:1, 1:1, 1:2, 1:3 and 1:4, respectively, and repeat the above two steps;

finally, according to the stress–strain relationship of different coal–rock height ratio samples, characteristics of energy accumulation and release during the deformation and failure process of coal–rock composite samples were calculated. The influence of coal–rock height ratios on mechanical behavior and energy evolution of test samples is obtained.

Results and analysis

Effect of coal-rock height ratios on strength and deformation

The full stress–strain curves of the coal-rock composite samples were obtained at different coal–rock height ratios, and mechanical parameters, such as elastic modulus, peak stress and corresponding deformation, were determined to explore the differences in mechanical parameters and mechanical behavior of coal–rock composite samples at different coal-rock height ratios. Figure 6a is uniaxial compressive stress–strain curve of coal–rock composite samples with different coal–rock height ratios. Figure 6b shows relationship between the uniaxial compressive strength (UCS), elastic modulus, and peak strain of the coal–rock composite samples with different coal–rock height ratios. The elastic modulus, peak stress, and corresponding deformation of different coal-rock height ratios samples are listed in Table 3.

From Fig. 6a, it can be seen that stress–strain curve of coal-rock composites with different coal–rock height ratios

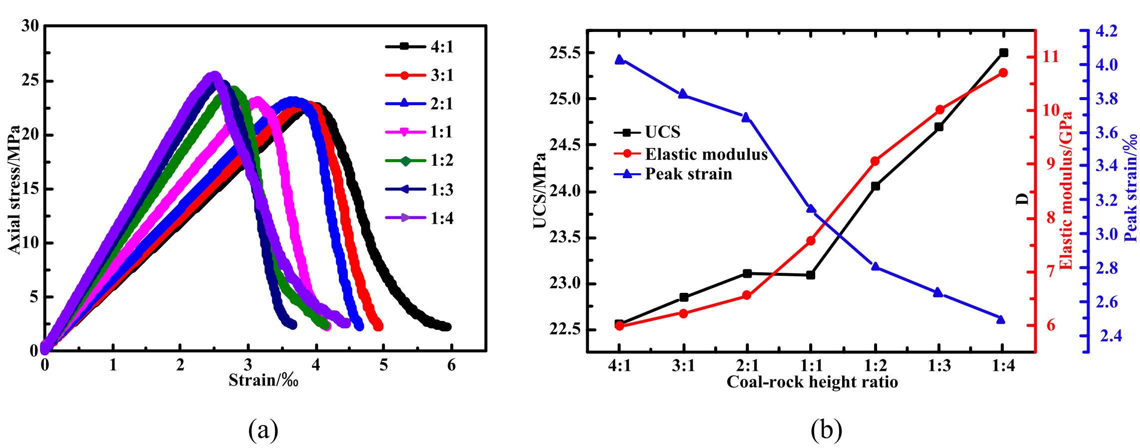

Fig. 6 Axial stress–strain curves and mechanical parameters for different coal–rock height ratios samples. **a** Axial stress vs. strain curves. **b** Elastic modulus, peak stress, and corresponding strain

Table 3 Numerical simulation results of uniaxial compression of coal–rock composites

Coal-rock height ratios	Uniaxial compression strength /MPa	Elastic modulus / GPa	Peak strain /‰
4:1	22.56	5.99	4.03
3:1	22.84	6.24	3.82
2:1	23.08	6.55	3.69
1:1	23.10	7.58	3.14
1:2	24.05	9.06	2.80
1:3	24.70	10.03	2.65
1:4	25.50	10.73	2.50

under uniaxial compression is roughly divided into four stages: linear elastic deformations, nonlinear deformations, post-peak strain softening, and residual deformations. The overall trend is not affected by the coal–rock height ratios, but it affects axial strain value corresponding to each stage. From Table 3 and Fig. 6b, it can be seen that as the rock height in coal–rock combination increases, the uniaxial compressive strength, peak strain and elastic modulus of the combination are different. This shows that coal–rock height ratios affect uniaxial compressive strength, peak strain and elastic modulus of the composite samples.

When coal–rock height ratios was reduced from 4:1 to 1:4, peak strengths of coal–rock composite samples with different height ratios increased by 1.24%, 1.05%, 0.09%, 6.06%, 2.70% and 3.24%, respectively. The increase rate is small. This shows that effect of different height ratios of coal and rock on the peak strength of the composite samples is weak. When coal–rock height ratios was reduced from 4:1 to 1:4, elastic modulus of coal–rock composite samples increased by 4.17%, 4.97%, 15.73%, 19.53%, 10.71% and 6.98%, respectively. When coal–rock height ratios change from 3:1 to 1:3, increase of the elastic modulus of the composite sample is larger. Especially when coal–rock height ratios decrease from 1:1 to 1:2, increased trend of elastic modulus reaches 19.53%. This is mainly because elastic modulus of rock is much larger than that of coal. When the proportion of coal decreases, its elastic modulus increases rapidly. Unlike uniaxial compressive strength and elastic modulus, when coal–rock height ratios are reduced from 4:1 to 1:4, peak strain of coal–rock composites with different height ratios show a decreasing trend. It decreased by 5.21%, 3.40%, 14.91%, 10.83%, 5.36% and 5.66%, respectively. It can be concluded from the above that the overall trend of the influence of the coal–rock height ratios on the uniaxial compressive strength, elastic modulus and peak strain of the composites is that with decrease of the coal–rock height ratios, uniaxial compressive strength and elastic modulus increase exponentially, while peak strain decreases approximately linearly. But the trend of increasing or decreasing is not the same.

Effect of coal–rock height ratios on failure patterns

The failure patterns of the coal–rock composite samples with different coal–rock height ratios are shown in Fig. 7. It can

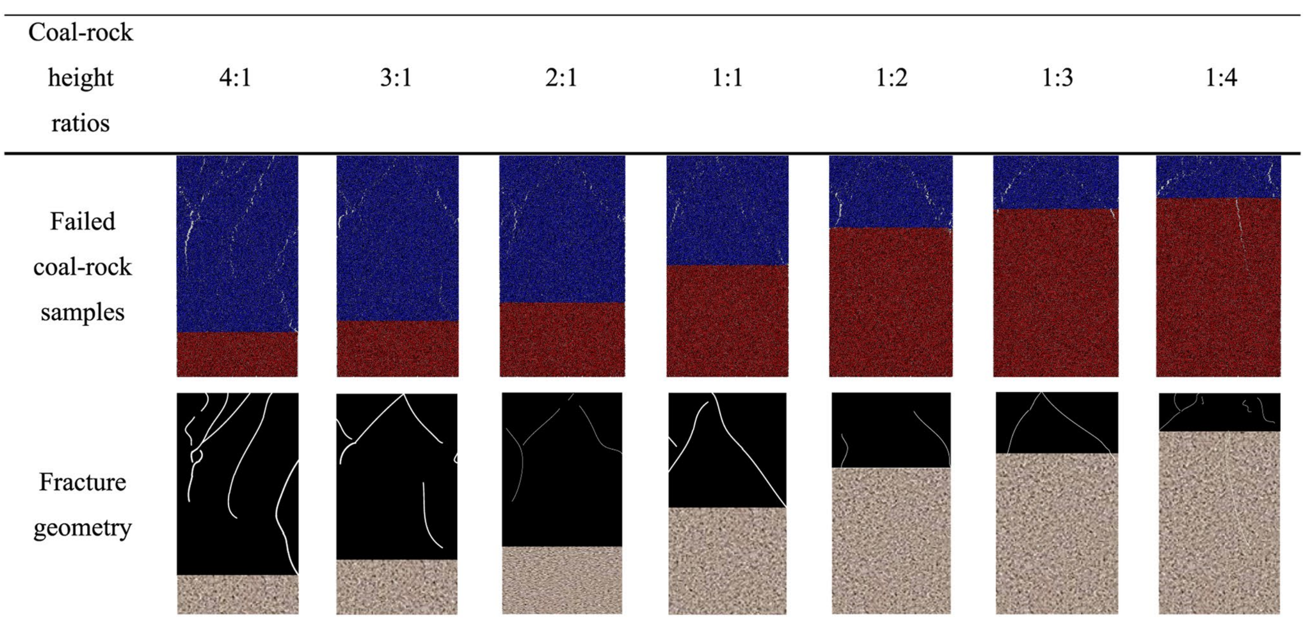

Fig. 7 Failed coal–rock composite sample and its fracture geometries

be seen from Fig. 7 that failure the coal–rock composites with different coal–rock height ratios mainly occurred in coal body, and rock body did not undergo significant damage. But as the coal–rock height ratios decreases, cracks also occur in rock body. When it is reduced to 1:3, cracks in coal body cause damage to the left and right sides of rock body near joint surface. When it is reduced to 1:4, coal body cracks propagate along the left and right upper sides of coal body, and an obvious crack is generated in rock body at the center to the left.

It can also be seen from Fig. 7 that failure mode of the coal–rock composite samples is complex failure. Shear failure is the main mode. The formation of multiple failure surfaces causes the final overall destruction of composites. When the height ratio is 4:1, coal body is more broken. When the height ratio is reduced from 4:1 to 1:3, the degree of coal body fragmentation gradually decreases. And coal body failure mode is mainly "V" type. When the coal–rock height ratios reduced to 1:4, failure mode is no longer "V" type. The degree of coal body fragmentation has increased, and rock body in the composites has also been damaged.

Effect of coal–rock height ratios on AE characteristics

Figure 8 shows stress and AE variation with strain curves in the process of deformation and failure of coal–rock composite samples under the uniaxial compression. It can be seen from Fig. 8 that under uniaxial compression conditions, changing trend of AE event counts during deformation and failure of coal–rock composites under different coal–rock height ratios are basically same. The number of AE event counts of coal–rock composites at different coal–rock height ratios is also roughly divided into four stages corresponding to the stress–strain curve of coal–rock composites.

Under uniaxial compression, initial stage of loading is the stage of linear elastic deformation. At this stage, in the state where stress of coal-rock composite sample is relatively small, original cracks in coal–rock composites are closed, and basically no new cracks occur. So the AE event count is less. This stage is called “quiet stage” (OA) of AE event count. With increase of loading stress, primary cracks in the coal–rock composites expand, and secondary cracks form and propagate. AE event count increases gradually. This stage is called "slow increase stage" (AB) of AE event count. When stress reaches the peak strength, crack rapidly propagates through. At this stage, AE event count also reached the maximum value. This stage is called “burst stage” (BC) of AE event count. As loading continues, new cracks will form due to residual strength. By the time loading was completed, internal cracks in the coal–rock composite samples penetrated, macro-cracks formed, and number of cracks gradually decreased. This stage is called “falling back stage” (CD) of AE event count. It can be seen from Fig. 8 that regardless of height ratios of coal and rock, there is an AE event count “slow increase stage” before the “burst stage” of AE event count. Therefore, the number of AE event counts during the AE “slow increase stage” of coal–rock composites with different height ratios suddenly increases, which can be used as the precursor information of coal–rock composites failure.

It can also be seen from Fig. 8 that as the coal–rock height ratios decreases, peak AE event counts increase first and then decrease. The main reason is that for the composite body, due to large difference in strength of coal body and the rock body, AE mainly occurs in coal body, and number of AE event counts decreases with decrease of the coal height.

Effect of coal–rock height ratios on energy accumulation and dissipation

The destruction of any substance is closely related to its energy change. Material destruction is essentially a state instability phenomenon driven by energy (Mikhalyuk and Zakharov, 1997; Xie et al. 2005). Therefore, energy theory can be used to study deformation and failure laws of coal–rock composites with different coal–rock height ratios, which is helpful for understanding mechanical behavior of coal–rock composites with different coal–rock height ratios. In fact, in various rock projects, the mining, disturbance and transformation of rock masses are always accompanied by energy input, accumulation, dissipation and release. However, considering the irreversibility of dissipative energy and the reversibility of elastic energy, this paper only considers change law of input energy, elastic strain energy and dissipation energy of coal–rock composites with different height ratios. External energy input causes energy dissipation such as damage and plastic deformation in rock or coal. Energy dissipation reduces rock or coal strength. On the other hand, increase in elastic energy accumulated in rock or coal increases rock or coal’s ability to resist damage. In other words, damage and destruction of rock or coal is a process of energy accumulation and dissipation. A rock mass unit deforms under action of an external force, assuming that physical process has no heat exchange with the outside world. It is a closed system. According to law of thermodynamics (Xie et al. 2005; Zhang 2013; Zhang et al. 2018; Hou et al. 2019):

$$U = U^d + U^e, \tag{1}$$

where $_U$ is the input energy from the external environment, U^e is the elastic energy accumulated inside the rock, U^d is the dissipated energy during deformation and damage process of rock, and correlation is shown in Fig. 9 (Xie et al. 2005; Zhang 2013; Zhang et al. 2018; Hou et al. 2019).

Fig. 8 AE event counts of coal–rock composite samples with different coal–rock height ratios

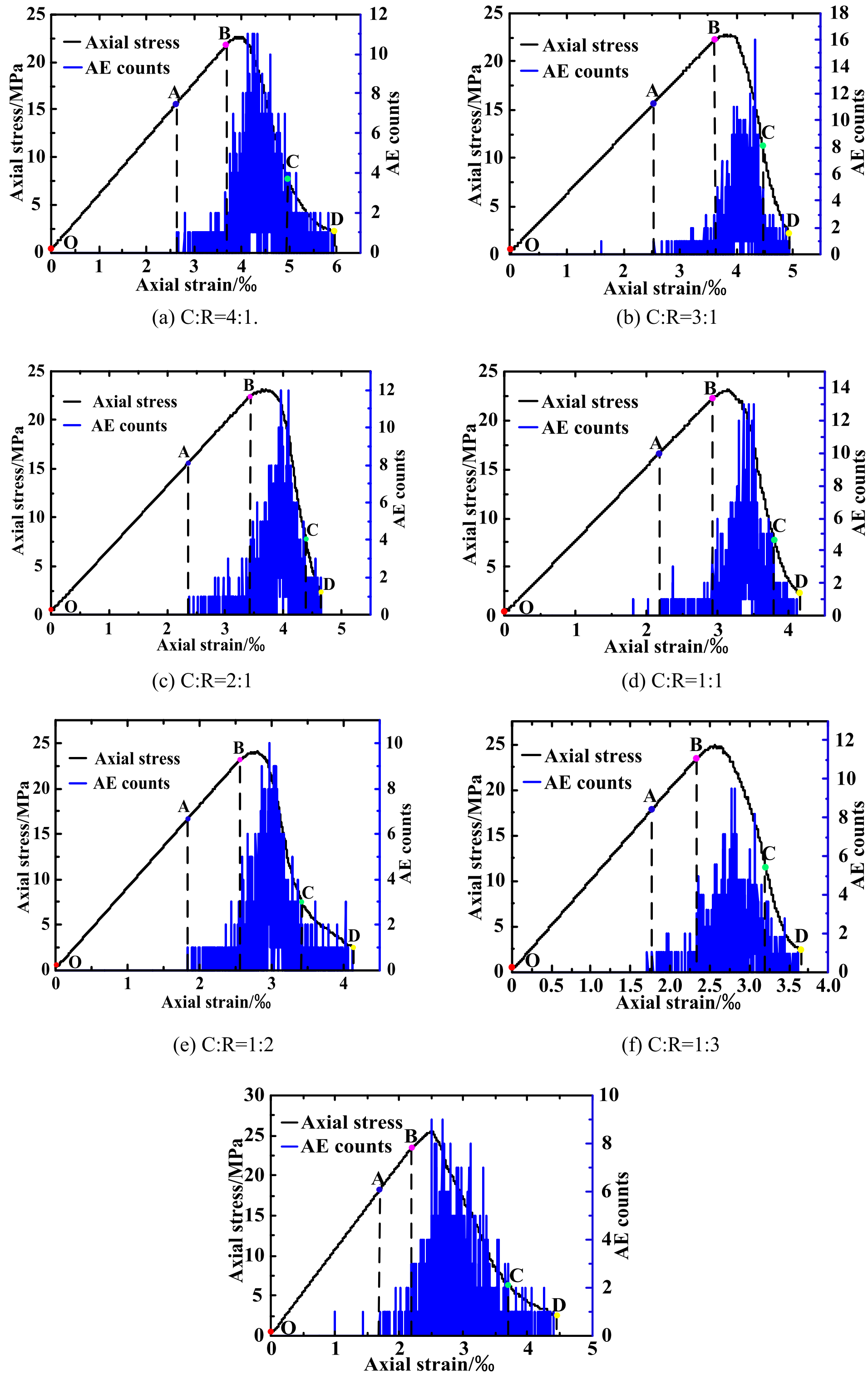

(a) C:R=4:1.

(b) C:R=3:1

(c) C:R=2:1

(d) C:R=1:1

(e) C:R=1:2

(f) C:R=1:3

(g) C:R=1:4

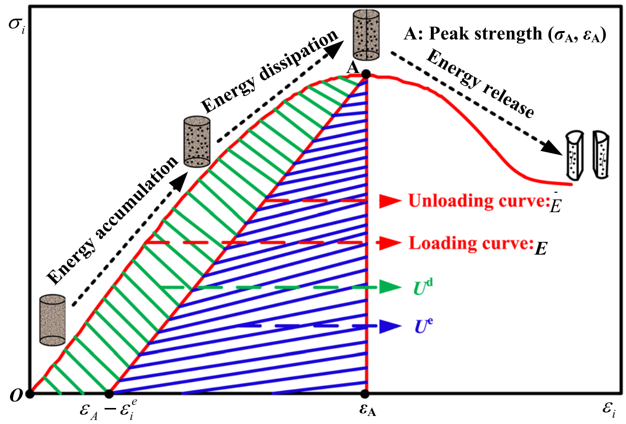

Fig. 9 Relationship between dissipative energy and releasable elastic strain energy in rock (Xie et al. 2005; Zhang 2013; Zhang et al. 2018; Hou et al. 2019)

As shown in Fig. 9, the shaded area U^e is the elastic strain energy stored in the rock due to elastic deformation. U^d is the dissipated energy associated with rock damage and plastic deformation. It includes surface energy caused by crack growth and plastic deformation energy caused by plastic damage and deformation. The equation for calculating energy of a rock element under triaxial stress is shown below (Xie et al. 2005; Zhang 2013; Zhang et al. 2018; Hou et al. 2019):

$$U = \int_0^{\varepsilon_1} \sigma_1 d\varepsilon_1 + \int_0^{\varepsilon_2} \sigma_2 d\varepsilon_2 + \int_0^{\varepsilon_3} \sigma_3 d\varepsilon_3 \tag{2}$$

$$U^e = \frac{1}{2\bar{E}}\left[\sigma_1^2 + \sigma_2^2 + \sigma_3^2 - 2\bar{\upsilon}\left(\sigma_1\sigma_2 + \sigma_2\sigma_3 + \sigma_1\sigma_3\right)\right], \tag{3}$$

where $\bar{E}$ and $\bar{\upsilon}$ are the average values of the unloading elastic modulus and Poisson's ratios, respectively.

Equation (4) is the calculation formula for releasable elastic strain energy during triaxial compression. When rock undergoes uniaxial compression ($\sigma_2 = \sigma_3 = 0$), Eq. (4) becomes:

$$U^e = \frac{\sigma_1^2}{2\bar{E}} \tag{4}$$

For different coal–rock height ratios composite samples, based on equations described above, energy components $_U$, U^e and U^d can be calculated directly from the experimental stress–strain curves. Figure 10 shows the change of $_U$, U^d and U^e for coal–rock composite samples. And it can be seen, energy evolution curves at different coal-rock height ratios exhibit similar trends: most of $_U$, U^d and U^e curves increase slowly first, fast afterwards and changed very sharply at peak stress points. Consistent with change trend of stress–strain curve of composites, energy evolution curve of coal–rock composites can also be divided into four stages. As shown in Fig. 10d, take coal–rock height ratios = 1:1 for example (points a_1, a_2 and a_3 are shown on the X-axis of Fig. 10d):

Stage 1: Linear elastic deformation stage ($\varepsilon_1 < a_1$): $_U$, U^e increased non-linearly. U^d increased linearly, but the increase was small.

Stage 2: Nonlinear deformation stage ($a_1 < \varepsilon_1 < a_2$): The total energy $_U$ and elastic strain energy U^e continue to increase linearly with strain. U^d still increases linearly. At this time, micro-cracks in the composites have been completely closed, and total input energy is basically converted into elastic strain energy of coal–rock composite sample. At this time, energy dissipation is very small.

Stage 3: Yield stage ($a_2 < \varepsilon_1 < a_3$): Total input energy $_U$ and elastic strain energy U^e continue to increase with deformation. But the rate of increase of elastic strain energy U^e gradually decreases. Elastic strain energy at peak strength reaches 351.70 KJ/m^3. Dissipated energy U^d starts to increase from a steady state, and the rate of increase gradually increases. The main reason is that new micro cracks gradually develop inside the coal–rock composites. With continuous development of deformation, the number of micro–cracks continues to increase, and input energy is dissipated by surface energy of micro–cracks, which causes the dissipation energy to begin to increase rapidly.

Stage 4: Post peak residual stage ($\varepsilon_1 > a_3$): After peak strength, the increase rate of total input energy $_U$ in the composites slows down, and elastic strain energy U^e decreases rapidly. And dissipated energy U^d increases rapidly and then gradually decreases. The final dissipated energy U^d exceeds elastic strain energy U^e. After elastic strain energy U^e stored in composites reaches the energy storage limit, due to generation of macroscopic cracks, it is quickly released in the form of kinetic energy, crack surface energy- and frictional energy.

To compare the energy evolution of coal–rock composite samples with different coal–rock height ratios directly, energy evolution curves are plotted in a single figure, as shown in Fig. 11. As it can be seen from Fig. 11a, the total input energy of the coal–rock composite samples increases approximately linearly with strain. The maximum value of total input energy of coal–rock composites decreased first and then increased with decrease of the coal–rock height ratios. When the coal–rock height ratio is reduced from 4:1 to 1:1, the maximum value of total input energy shows a decreasing trend. When decreasing from 1:1 to 1:4, the maximum value of total input energy shows an increasing trend. With decreasing the coal–rock height ratios, the accumulated elastic energy rises up more rapidly before the peak strength (Fig. 11b), and the peak value decreases as well, reaching a minimum of 301.93 KJ/m^3 at the coal–rock height ratios 1:4 reaching a maximum of 426.68 KJ/m^3 at 4:1 (Fig. 11b). After the peak strength, regardless of the height

Fig. 10 Energy evolution curves of coal-rock composite samples with different coal–rock height ratios ($_U$ the total absorbed energy, U^e the recoverable elastic strain energy, U^d the dissipated energy)

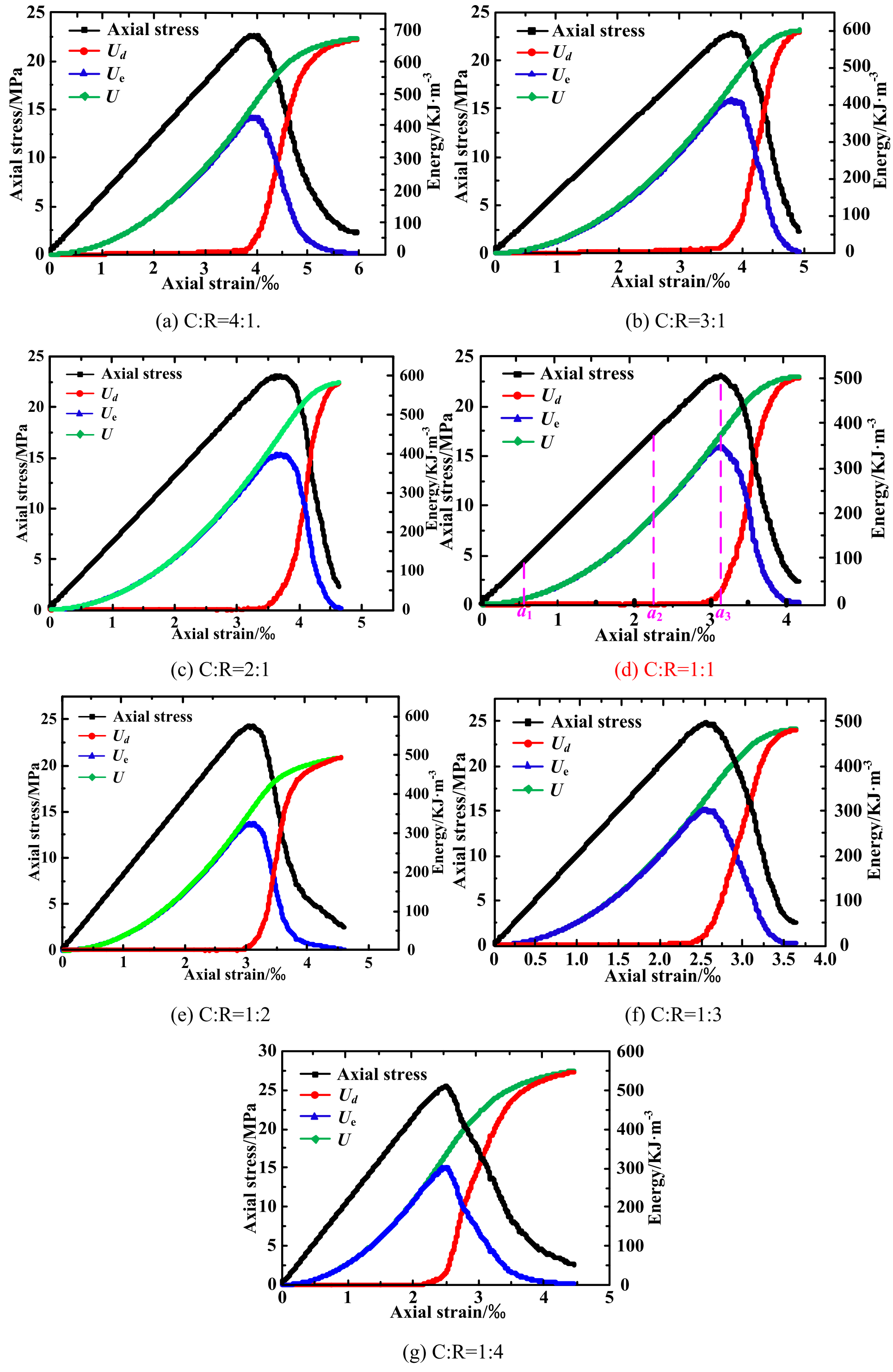

ratios of coal and rock, the accumulated elastic strain energy rapidly decreases until it disappears after test. In addition, the dissipated energy of coal–rock composites gradually increases with decrease of the coal–rock height ratios, and the peak dissipated energy value decreases first and then increases (Fig. 11c), reaching a minimum of 26.32KJ/m^3 at 1:3. It shows that with the decrease of the coal–rock height ratios, the internal structure changes caused by the dissipated energy will decrease first and then increase. Especially during the post-peak failure process, cracks in the coal–rock composites have larger propagation and aggregation. From the perspective of energy evolution, it is revealed that the damage is more serious when the coal body is relatively large or small.

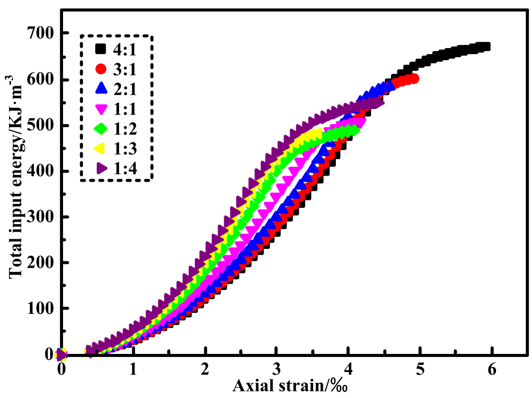

(a) Total input energy U

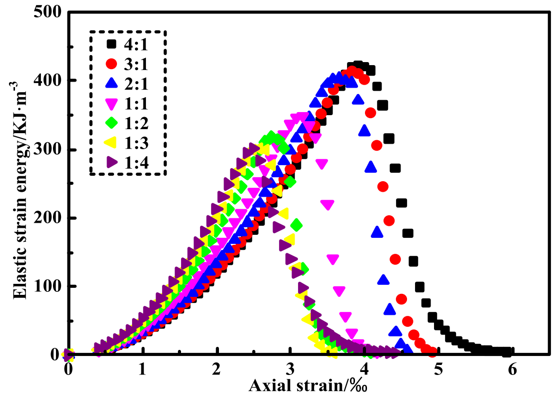

(b) The elastic strain energy U^e

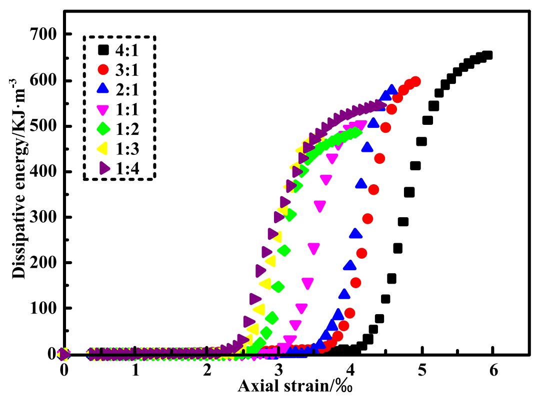

(c) The dissipative energy U^d

Fig. 11 Relationship between energy and strain of coal–rock composite samples with different coal–rock height ratios

According to the change of energy and strain of coal–rock composites with different coal–rock height ratios, the evolution characteristics of energy are further discussed. The total input energy $_U$, recoverable elastic strain energy U^e and dissipated energy U^d at the peak point of stress–strain curve are designated as U_A, U_A^e and U_A^d, respectively. The relationships between U_A, U_A^e U_A^d and height ratios are illustrated in Fig. 12. The values of U_A, U_A^e and U_A^d at peak strength are shown in Table 4.

From Table 4 and Fig. 12, it can be seen that the accumulation and dissipation of energy are closely related to the coal–rock height ratios. The trends of U_A and U_A^d with coal–rock height ratios are the same. As the coal–rock height ratios decrease, U_A and U_A^d decrease first and then increase. As the coal–rock height ratios decrease from 4:1 to 1:4, U_A decreases from 467.81 to 331.73 KJ/m^3, then increases from 331.73 to 338.34 KJ/m^3, U_A^d decreases from 41.13 to 26.32 KJ/m^3, then increases from 26.32 to 36.41 KJ/m^3, respectively. Unlike U_A and U_A^d, U_A^e tends to decrease approximately linearly with decreasing coal-rock height ratios. When it is reduced from 4:1 to 1:4, its value is reduced from 426.68 to 301.93 KJ/m^3. As shown in Table 4, as the coal–rock height ratios decreases, U_A^e / U_A increases first and then decreases. U_A^e / U_A increases from 91.2% to 92.7% first, then decreases from 92.7 to 89.2%. However, U_A^d / U_A tends to decrease first and then increase. U_A^d / U_A decreases from 8.8 to 7.3% first, then increases from 7.3 to 10.8%. The results show that the energy dissipation is relatively large as the coal proportion is relatively large or small. The dissipation of energy is closely related to the formation of internal cracks. Once again, from the view of energy evolution, it shows that the destruction of composites is more serious when the proportion of coal body is larger or smaller.

Conclusions

This paper presented the results of a study of height ratios on the mechanical and energy characteristics of coal–rock composite samples using numerical simulation tests. It was found that coal–rock height ratios had significant effects

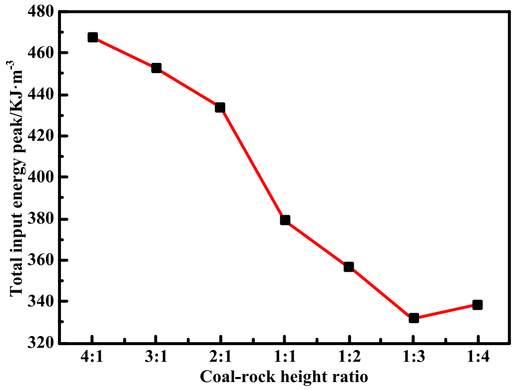

(a) Total input energy U_A at peak point

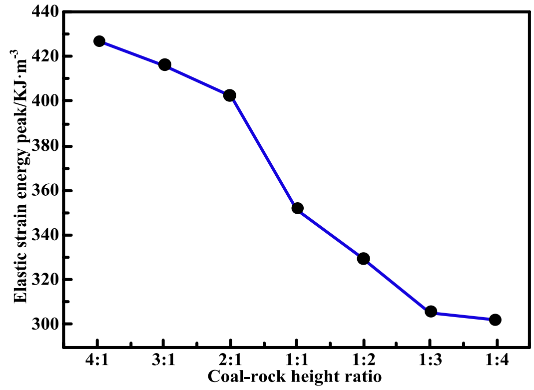

(b) The elastic strain energy U^e at peak point

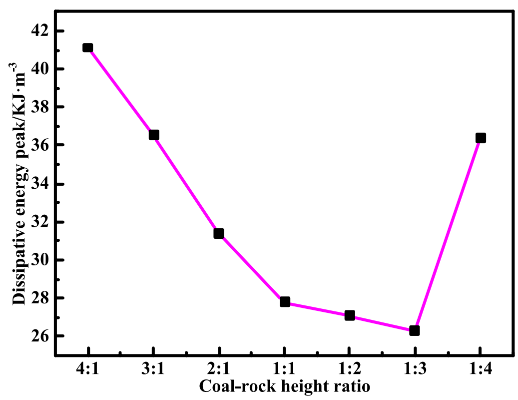

(c) The dissipative energy U^d at peak point

Fig. 12 The relationships between U_A, U_A^e, U_A^d and coal–rock height ratios

Table 4 U_A, U_A^e and U_A^d at the peak strength with different coal–rock height ratios

Coal-rock height ratios	U_A (KJ/m^3)	U_A^e (KJ/m^3)	U_A^d (KJ/m^3)	U_A^e/U_A	U_A^d/U_A
4:1	467.81	426.68	41.13	0.912	0.088
3:1	452.45	415.92	36.53	0.919	0.081
2:1	433.92	402.54	31.38	0.928	0.072
1:1	379.47	351.70	27.77	0.927	0.073
1:2	356.46	329.41	27.05	0.924	0.076
1:3	331.73	305.41	26.32	0.921	0.079
1:4	338.34	301.93	36.41	0.892	0.108

on mechanical behavior and energy evolution of coal–rock composite samples. The following are main conclusions derived from this study:

(1) The smaller coal–rock height ratios, the larger elastic modulus and peak strength of coal–rock composite samples, while axial strain at peak stress seems to decrease linearly with decrease of coal–rock height ratios. And the elastic modulus and peak strength increased exponentially with the decrease of coal–rock height ratios.

(2) The failure modes of test samples changed significantly with the decreasing of coal–rock height ratios. When the coal–rock height ratio is 4:1, the coal body is more fragmented. When the height ratio is reduced to 1:3, the degree of coal body fragmentation gradually decreases, and failure mode is mainly "V" failure. When it is reduced to 1:4, the failure mode is no longer "V", and the degree of coal body fragmentation is increased, and the rock body in the composites is also damaged.

(3) During uniaxial compression failure process of the coal–rock composites, the number of AE event counts all experienced four stages: "quiet stage", "slow increase stage", "burst stage" and "falling back stage". And with the decrease of coal–rock height ratios, the number of AE event counts of composites increased first and then decreased.

(4) The energy accumulation and dissipation of coal–rock composite samples are closely related to coal–rock height ratios. The $_U$, U^e and U^d at different coal–rock height ratios exhibited similar trends, all of which increase slowly first, fast afterwards and very sharply at the peak stress points. And values of U_A and U_A^d decrease firstly, then increase as coal-rock height ratios decreases and value of U_A^e decrease as the coal-rock height ratios decreases. While decrease of both U_A and U_A^d are larger than U_A^e. What is more, when coal–rock height ratios decrease, U_A^e/U_A increases first and then decreases. U_A^e/U_A increases from 91.2% to 92.7% first, then decreases from 92.7% to 89.2%. However, U_A^d/U_A tends to decrease first and then increase. U_A^d/U_A decreases from 8.8% to 7.3% first, then increases from 7.3 to 10.8%.

(5) In this paper, the mechanical and energy characteristics of coal–rock composite samples are studied in detail through numerical simulation test. However, only simulation and experimental research of small-scale composite test samples in laboratory are currently performed, and research on field scale is yet to be performed. In addition, influence of coal and rock heterogeneity and joints are not considered in numerical simulation. So more research work need to be done to understand this issue.

Acknowledgements This study was financially supported by National Key R&D Program of China (Grant No. 2018YFC0604703), the National Natural Science Foundation of China (Grant No. 51774196, No. 51804181, No. 51874190), Key R&D Program of Shandong Province (No. 2019GSF111020), Major Program of Shandong Province Natural Science Foundation (No. ZR2018ZA0603), Shandong Province Natural Science Fund (No. ZR2018QEE002). The first author would like to thanks for financial support by the CSC.

References

Álvarez-Fernández MI, González-Nicieza C, Álvarez-Vigil AE, HerreraGarcía G, Torno S (2009) Numerical modeling and analysis of the influence of local variation in the thickness of a coal seam on surrounding stresses: application to a practical case. Int J Coal Geol 79:157–166

CESA (2019) Metallurgical Industry Energy Saving Committee of China Energy Saving Association (CESA). China's steel industry energy saving and low carbon development report in 2019

Chen YL, Wu HS, Zhang MW, Wu Y, Zhang HQ, Zhang GM (2016) Research on the upper protective coal seam mining effect induced by coal thickness and inter burden rock properties. J Min Saf Eng 33(4):578–584

Chen YL, Zuo JP, Liu DJ, Wang ZB (2018) Deformation failure characteristics of coal-rock combined body under uniaxial compression: experimental and numerical investigations B. Eng Geol Environ 3:1–16

Chen SJ, Yin DW, Jiang N, Wang F, Zhao ZH (2019) Mechanical properties of oil shale-coal composite samples. Inter J Rock Mech Min Sci 123:104120

Cheng ZB, Li LH, Zhang YN (2019) Laboratory investigation of the mechanical properties of coal-rock combined body. Bull Eng Geol Environ 79:1947–1958

Cho N, Martin CD, Sego DC (2007) A clumped particle model for rock. Int J Rock Mech Min Sci 44(7):997–1010

Cundall PA, Strack ODL (1980) Discussion: a discrete numerical model for granular assemblies. Géotechnique 30(3):331–336

Gong FQ, Ye H, Luo Y (2018) The effect of high loading rate on the behavior and mechanical properties of coal-rock combined body. Shock Vib. https://doi.org/10.1155/2018/4374530

Guo WY, Tan YL, Yu FH, Zhao TB, Hu SC, Huang DM, Qin ZW (2018) Mechanical behavior of rock-coal-rock specimens with different coal thicknesses. Geomech Eng 15(4):1017–1027

Hou ZK, Gutierrez M, Ma SQ, Almrabat A, Yang CH (2019) Mechanical behavior of shale at different strain sates. Rock Mech Rock Eng 52(10):3531–3544

Hu SC, Tan YL, Zhou H, Ru WK, Ning JG, Wang J, Huang DM, Li Z (2019) Anisotropic modeling of layered rocks incorporating planes of weakness and volumetric stress. Energy Sci Eng 00:1–15

Huang WP, Li C, Zhang LW, Yuan Q, Zheng YS, Liu Y (2018) In situ identification of water-permeable fractured zone in overlying composite strata. Inter J Rock Mech Min Sci 105:85–97

Kenetia A, Sainsbury BA (2018) Review of published rockburst events and their contributing factors. Eng Geol 246:361–373

Liu SH, Mao DB, Qi QX, Li FM (2014) Under static loading stress wave propagation mechanism and energy dissipation in compound coal-rock. J China Coal Soc 39(S1):15–22

Liu XS, Ning JG, Tan YL, Gu QH (2016) Damage constitutive model based on energy dissipation for intact rock subjected to cyclic loading. Int J Rock Mech Min Sci 85:27–32

Liu XS, Tan YL, Ning JG, Lu YW, Gu QH (2018) Mechanical properties and damage constitutive model of coal in coal-rock combined body. Inter J Rock Mech Min Sci 110:140–150

Lockner DA (1993) The role of acoustic emission in the study of rock fracture. Int J Rock Mech Min Sci Geomech Abstr 30(7):883–899

Ma Q, Tan YL, Liu XS, Gu QH, Li XB (2020) Effect of coal thicknesses on energy evolution characteristics of roof rock-coal-floor rock sandwich composite structure and its damage constitutive model. Compos Part B-Eng 198:108086

Mansurov VA (1994) Acoustic emission from failing rock behavior. Rock Mech Rock Eng 27(3):173–182

Mikhalyuk AV, Zakharov VV (1997) Dissipation of dynamic-loading energy in quasi-elastic deformation processes in rocks. J App Mech Tech Phys 38(2):312–318

Mishra B, Verma P (2015) Uniaxial and triaxial single and multistage creep tests on coal-measure shale rocks. Int J Coal Geol 137:55–65

Ning JG, Wang J, Tan YL, Xu Q (2020) Mechanical mechanism of overlying strata breaking and development of fractured zone during close-distance coal seam group mining. Int J Min Sci Technol 30(2):207–215

Poulsen BA, Shen BT, Williams DJ, Huddlestone-Holmes C, Erarslan N, Qin J (2014) Strength reduction on saturation of coal and coal measures rocks with implications for coal pillar strength. Int J Rock Mech Min Sci 71:41–52

Sun W, Zhang Q, Luan YZ, Zhang XP (2018) A study of surface subsidence and coal pillar safety for strip mining in a deep mine. Environ Earth Sci 77:627

Tan YL, Guo WY, Gu QH, Zhao TB, Yu FH, Hu SC, Yin YC (2016) Research on the rock burst tendency and AE characteristics of inhomogeneous coal-rock combination bodies. Shock Vib. https://doi.org/10.1155/2016/9271434

Tan YL, Liu XS, Shen BT, Ning JG, Gu QH (2018) New approaches to testing and evaluating the impact capability of coal seam with hard roof and/or floor in coal mines. Geomech Eng 14(4):367–376

Tan YL, Fan DY, Liu XS, Song SL, Li XF, Wang HL (2019a) Numerical investigation on failure evolution of surrounding rock for super-large section chamber group in deep coal mine. Energy Sci Eng 7:3124–3146

Tan YL, Guo WY, Xin HQ, Zhao TB, Yu FH, Liu XS (2019b) Key technology of rock burst monitoring and control in deep coal mining. J China Coal Soc 44(01):167–179

Thomas L (2002) Coal geology. John Wiley and Sons, New York, p 384

Wang X, Tian LG (2018) Mechanical and crack evolution characteristics of coal-rock under different fracture-hole conditions: a numerical study based on particle flow code. Environ Earth Sci 77:297

Wang K, Du F, Zhang X, Wang L, Xin CP (2017) Mechanical properties and permeability evolution in gas-bearing coal-rock combination body under triaxial conditions. Environ Earth Sci 76(24):815

Wang CX, Shen BT, Chen JT, Tong WX, Jiang Z, Liu Y, Li YY (2020) Compression characteristics of filling gangue and simulation of mining with gangue backfilling: an experimental investigation. Geomech Eng 20(6):485–495

Ward CR (1984) Coal geology and coal technology. Blackwell Scientific Publications, Melbourne, p 345

Xie HP (2017) Research framework and anticipated results of deep rock mechanics and mining theory. Adv Eng Sci 49(2):1–16

Xie HP, Peng RD, Ju Y, Zhou HW (2005) On energy analysis of rock failure. Chin J Rock Mech Eng 24(15):2603–2608

Yang Z, Qi QJ, Ye DD, Li X, Luo H (2016) Variation of internal infrared radiation temperature of composite coal-rock fractured under load. J China Coal Soc 41(3):618–624

Yin DW, Chen SJ, Sun XZ, Jiang N (2019) Strength Characteristics of Roof Rock-coal Composite Samples with Different Height Ratiosunder Uniaxial Loading. Arc Min Sci 64(2):307–319. https://doi.org/10.24425/ams.2019.128685

Zhang ZZ (2013) Energy evolution mechanism during rock deformation and failure. China University of Mining and Technology, Beijing

Zhang XT, Dou LM (2006) Numerical simulation of the influence of coal seam hardness and thickness on rock burst. J Min Saf Eng 03:277–280

Zhang XP, Wong LNY (2012) Cracking processes in rock-like material containing a single flaw under uniaxial compression: a numerical study based on parallel bonded-particle model approach. Rock Mech Rock Eng 45:711–737

Zhang MW, Shimada H, Sasaoka T, Matsui K, Dou LM (2014) Evolution and effect of the stress concentration and rock failure in the deep multi-seam coal mining. Environ Earth Sci 72(3):629–643

Zhang Q, Zhang JX, Han XL, Ju F, Tai Y, Li M (2016) Theoretical research on mass ratio in solid backfill coal mining. Environ Earth Sci 75(7):586

Zhang YZ, Wang G, Jiang Y, Wang SG, Zhao HH, Jing WJ (2017) Acoustic emission characteristics and failure mechanism of fractured rock under different loading rates. Shock Vib 15(6):1–13

Zhang ZP, Xie HP, Zhang R, Zhang ZT, Gao MZ, Jia ZQ, Xie J (2018) Deformation damage and energy evolution characteristics of coal at different depths. Rock Mech Rock Eng 52:1491–1503

Zhang C, Liu JB, Zhao YX, Han PH, Zhang L (2020a) Numerical simulation of broken coal strength influence on compaction characteristics in goaf. Nat Resour Res 29(4):2495–2511

Zhang GC, Chen LJ, Wen ZJ, Chen M, Tao GZ, Li Y, Zuo H (2020b) Squeezing failure behavior of roof-coal masses in a gob-side entry driven under unstable overlying strata. Energy Sci Eng 8(7):2443–2456

Zhao YX, Jiang YD, Zhu J, Sun GZ (2008) Experimental study on precursory information of deformation and failure of coal rock combination. Chin J Rock Mech Eng 27(2):128–135

Zhao ZH, Wang WM, Wang LH, Dai CQ (2015) Compression-shear strength criterion of coal-rock combination model considering interface effect. Tunn Undergr Sp Tech 47(5):193–199

Zhao TB, Guo WY, Lu CP, Zhao GM (2016) Failure characteristics of combined coal-rock with different interfacial angles. Geomech Eng 11(3):345–359

Zhao ZH, Sun W, Zhang MZ, Gao XJ, Chen SJ (2020) Fracture mechanical behavior of cracked cantilever roof with large cutting height mining. Shock Vib. https://doi.org/10.1155/2020/1641382

Zhao ZH, Sun W, Chen SJ, Yin DW, Liu H, Chen BS (2021) Determination of critical criterion of tensile-shear failure in Brazilian disc based on theoretical analysis and meso-macro numerical simulation. Comput Geotech 134:104096. https://doi.org/10.1016/j.compgeo.2021.104096

Zuo JP, Xie HP, Wu AM, Liu JF (2011) Investigation on failure characteristics and mechanical behavior of deep coal-rock single body and combined body under different confining pressures. Chin J Rock Mech Eng 30(1):84–92